JOURNAL OF MATERIALS SCIENCE 29 (1994) 2513–2520

Effect of defects induced by doping and fast neutron irradiation on the thermal properties of lithium ammonium sulphate crystals

S. H. KANDIL; M. E. KASSEM*, A. M. EL-KHATIB*, T. A. RAMADAN, M. M. DARWISH
*Department of Materials Science, Institute of Graduate Studies and Research, and *Department of Physics, Faculty of Science, Alexandria University, Alexandria, Egypt*

Structural defects were introduced in lithium ammonium sulphate crystals (LAS) either in the process of crystal growth (in the form of foreign ions) or by neutron irradiation. The effect of such defects on the thermal properties of LAS crystals was studied in the temperature range 300–500 K. It was assumed that the doped LAS crystals are composed of a two-phase system having different thermal parameters in each phase. The specific heat at constant pressure, C_p, of irradiated samples was found to decrease with increasing irradiation doses. The thermal expansion of LAS crystals was found to be dependent on neutron irradiation, and was attributed to two processes: the release of new species and the trapping process.

1. Introduction

Lithium ammonium sulphate, $LiNH_4SO_4$ (LAS), is one member of the family of double sulphate crystals with the general formula $A_1A_2BX_4$ where A_1 denotes Li^+ or Na^+ ions, A_2 denotes Na^+, K^+, Rb^+, Cs^+ ions, NH_4^+ or $N_2H_5^+$ groups, and BX_4 denotes SO_4^{-2}, SeO_4^{-2} or BeF_4^{-2} groups. LAS is thus regarded as one of the ammonium sulphate-type ferroelectrics and it has been reported to exhibit an interesting sequence of structural phase transitions [1–3].

The α-phase ($T > 460$ K) of LAS crystals has orthorhombic symmetry with well-defined lattice constants, and well characterized structure [4–6]. The high-temperature phase transition at 460 K was suggested to be a first-order ferroelectric phase transition. This has been characterized by: (a) the discontinuity in spontaneous polarization [2]; (b) thermal hysteresis and the latent heat of transition [7]; and (c) discontinuities of the lattice parameters and the volume of the sample [8].

The room-temperature phase of LAS crystal, α-phase ($460 > T > 285$ K), was also reported to be orthorhombic and with well-defined lattice constants [2, 9].

Generally, defects can be introduced either during crystal growth (in the form of foreign ions) or by irradiation. Defects introduced by fast neutron irradiation consist of point defects, because here the main effect is due to the elastic collisions of fast neutrons from the neutron flux with lattice atoms. As a result of irradiation, the chemical bonds are damaged and various kinds of radicals are created [10–15].

The introduction of defects, even at low density, influences the most characteristic features of the crystal. In the case of ferroelectric crystals, the switchability of spontaneous polarization, anomalies in the physical properties at the Curie point, and the non-linear dielectric properties are found to be highly sensitive to defects. Moreover, the defect-induced changes were found to be dependent on whether the defects were introduced in the ferroelectric or paraelectric phase of the crystal.

The aim of this work was to study the influence of defects on the thermal properties of LAS. The changes in the thermal behaviour of LAS crystals in the vicinity of the phase-transition temperature due to doping, as well as fast neutron irradiations, were also studied.

2. Experimental procedure

Single crystals of lithium ammonium sulphate, $LiNH_4SO_4$, were grown by a slow evaporation method from aqueous solution containing equimolar amounts of pure $Li_2SO_4 \cdot H_2O$ and $(NH_4)_2SO_4$.

Specimens, in the form of rods (1 cm × 0.15 cm × 0.15 cm), were cut with edges parallel to the crystallographic axes from the formed single crystal of LAS using a wet thread saw.

Doped LAS crystals were also prepared by a slow evaporation method from an aqueous solution containing equimolar amounts of pure $Li_2SO_4 \cdot H_2O$ and the necessary amount of the dopant. The impurities selected for this study were copper, zinc and chromium ions. These ions were added to the growth solution of LAS as metal sulphates, with the required concentrations. The purity of the various sulphate dopants used were all in the 99% + range.

For irradiated samples, the neutron generator used was a Philips type PW 5310. It is a compact sealed-off accelerating tube with a built-in target that generates 15 MeV neutrons by the well-known (D–T) reaction.

0022-2461 © *1994 Chapman & Hall*

The prepared samples (which were cut with edges parallel to the crystallographic axes) were arranged around the D–T compact neutron source according to their crystallographic axes. The samples were irradiated for different periods to obtain different fluencies. The neutron flux from the source was determined by using the foil technique [16] and found to be 6×10^5 n cm^{-2} s^{-1}.

3. Results and discussion

3.1. Thermal properties of LAS crystals

LAS crystals doped with chromium, zinc and copper ions were studied using differential thermal analysis (DTA). Fig. 1 shows the DTA curves for LAS crystals doped with 0.0, 0.1, 0.5, 1.0 and 2.0 wt % chromium ions, as well as the DTA curve for pure $Cr_2(SO_4)_3$. It is clear that an endothermic peak in the temperature around 360 K has appeared in addition to the endothermic peak of the high-temperature phase transition at 460 K (I → II phase transition). The endothermic peak at 360 K was attributed to the decomposition of the chromic sulphate into the oxide in the same manner as the pure $Cr_2(SO_4)_3$ sample seen at about 335 K. The shift which occurred in the decomposition temperature to higher values for doped crystals could be attributed to the thermal diffusivity of the doped LAS crystals and to the heat transfer inside the sample.

Fig. 2 shows the DTA curves for LAS crystals doped with different weight per cents of zinc ions (0.0, 0.1 and 0.5%) as well as the DTA curve for pure $ZnSO_4 \cdot 7H_2O$ sample. The doped samples showed endothermic peaks which were attributed to dehydration of water of crystallization and melting of the dopant materials, in addition to the endotherm of the high-temperature phase transition at 460 K.

Fig. 3 shows the DTA curves for LAS crystals doped with different weight per cents of copper ions (0.0, 0.1, 0.5 and 1.0%) as well as the DTA curve for pure $CuSO_4 \cdot 5H_2O$ sample. The DTA curves of doped samples showed endothermic peaks correspond-

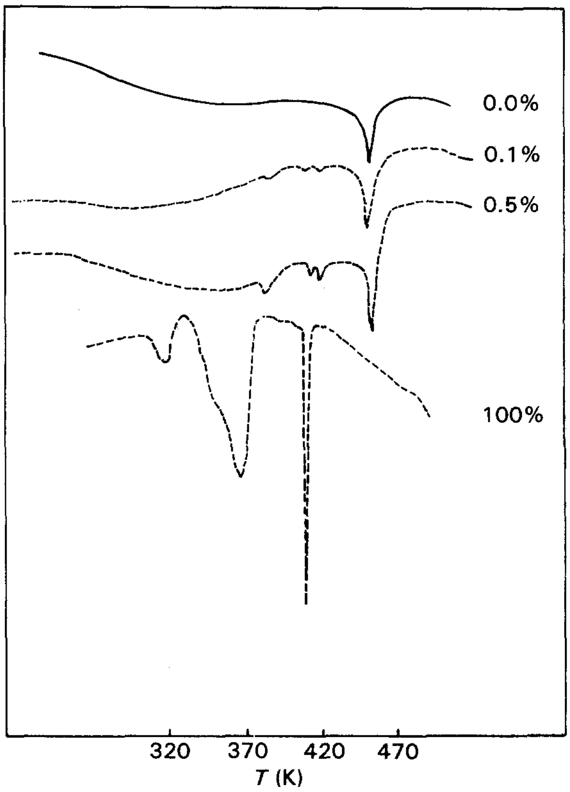

Figure 2 DTA curve of $LiNH_4SO_4$ crystal doped with Zn^{2+} ions.

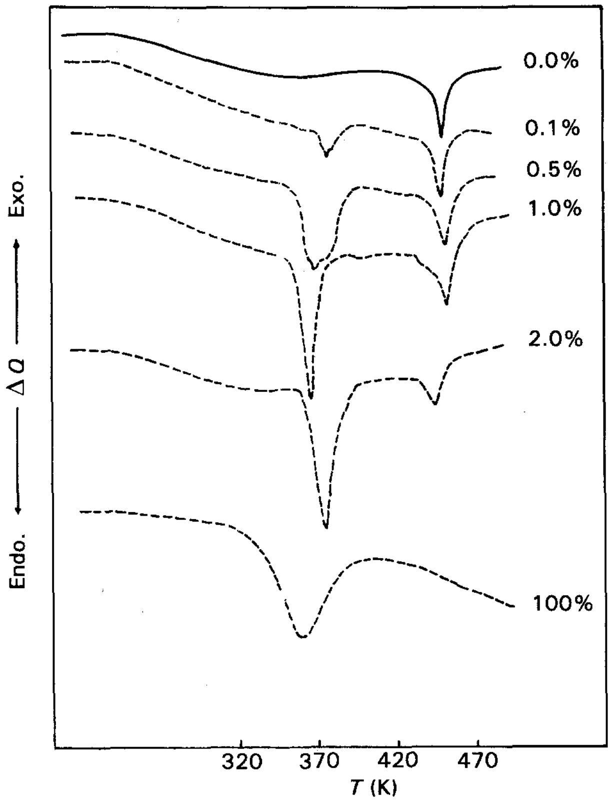

Figure 1 DTA curve of $LiNH_4SO_4$ crystal doped with Cr^{3+} ions.

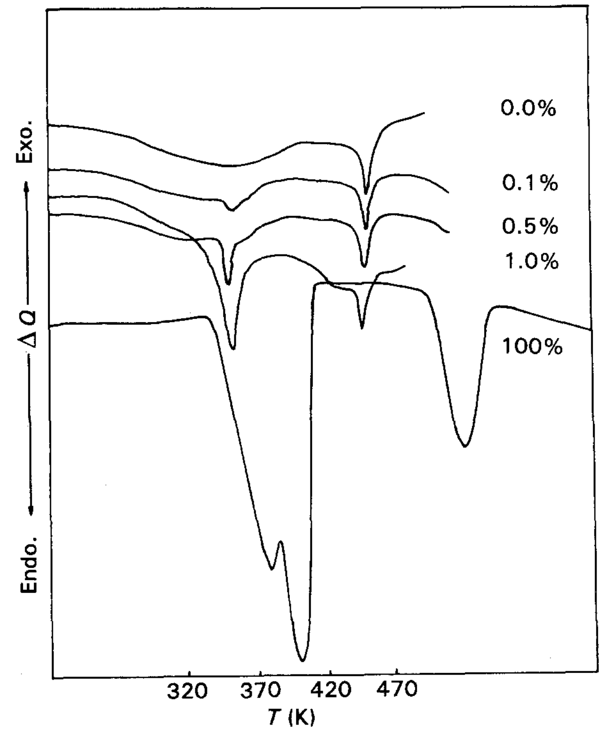

Figure 3 DTA curve of $LiNH_4SO_4$ crystal doped with Cu^{2+} ions.

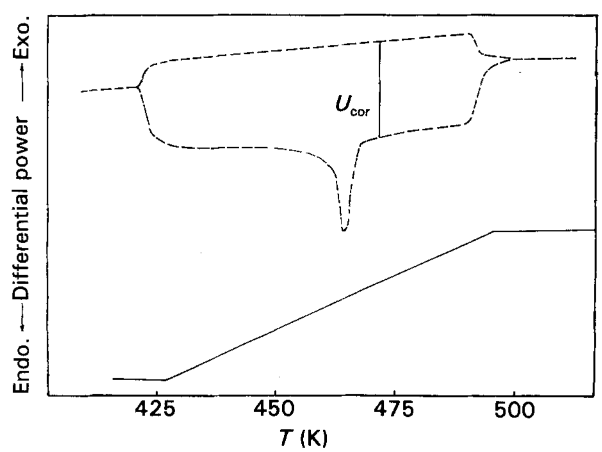

Figure 4 Corrected DSC curve of $[Li_x(NH_4)_{1-x}]_2SO_4$ crystal.

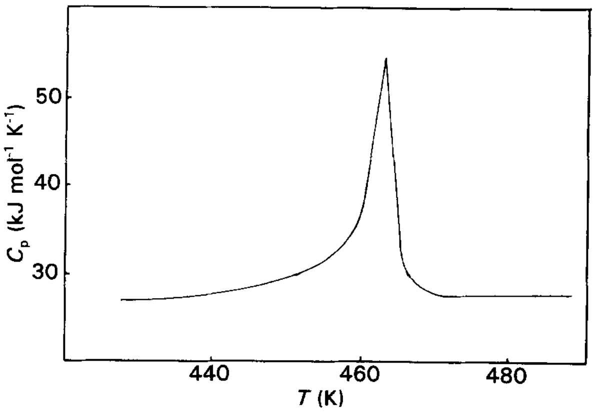

Figure 5 The temperature dependence of C_p of $LiNH_4SO_4$ crystal.

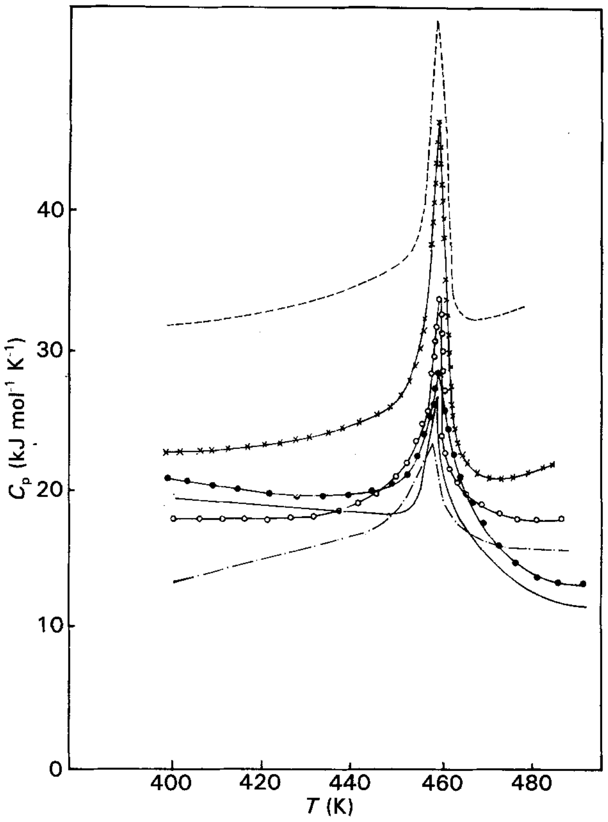

Figure 6 The temperature dependence of C_p for some irradiated $LiNH_4SO_4$ crystals. Dose (10^{10} n cm^{-2}): (----) 0, (×) 0.432, (○) 1.296, (●) 1.944, (——) 2.700, (—·—) 3.888.

TABLE I The $(C_p)_{max}$ of some irradiated $[Li_x(NH_4)_{1-x}]_2SO_4$, $x = 0.5$, crystal

Dose (10^{10} n cm^{-2})	C_p (J mol^{-1} K^{-1})
0	54.5
0.432	47.3
1.296	34.9
1.944	29.4
3.888	23.5

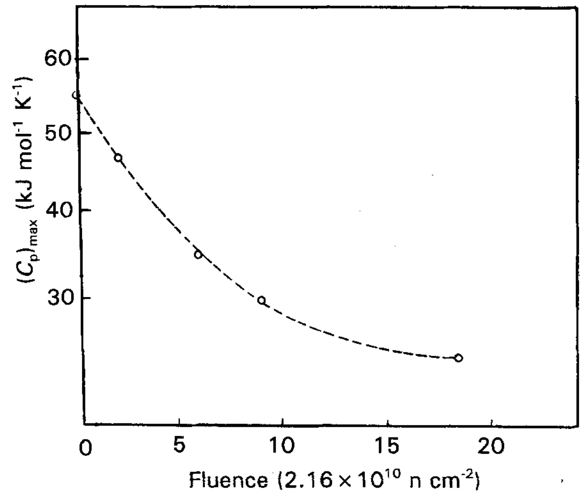

Figure 7 The change of C_p for some irradiated $LiNH_4SO_4$ crystals as a function of the irradiation dose.

TABLE II Thermodynamic data for some irradiated $[Li_x(NH_4)_{1-x}]_2SO_4$, $x = 0.5$, crystal

Dose (10^{10} n cm^{-2})	ΔH (J mol^{-1})	ΔS (J mol^{-1} K^{-1})
0	854	1.870
1.944	809	1.764
2.700	601	1.312
3.888	498	1.096

ing to the dehydration of water of crystallization (in the same manner as the pure $CuSO_4 \cdot 5H_2O$ sample) in addition to the endotherm of the I → II phase transition at 460 K.

In general, the impurities caused significant changes in the thermal properties of LAS crystals. The doping materials induced defects in the crystal structure which affected the thermal parameters of the crystals, because the thermal diffusivity is affected by the presence of foreign ions as well as the domain walls.

It is assumed that the doped crystals are composed of a two-phase system with different thermal parameters in each phase. One of the two phases contains the perfect LAS crystal lattice while the other contains the regions distorted by the presence of impurity ions (copper, zinc, chromium therein).

3.2. Effect of fast neutron irradiations on the thermal properties of LAS crystals

3.2.1. Specific heat, C_p

The specific heat at constant pressure, C_p, of the LAS crystals was measured in the temperature range of

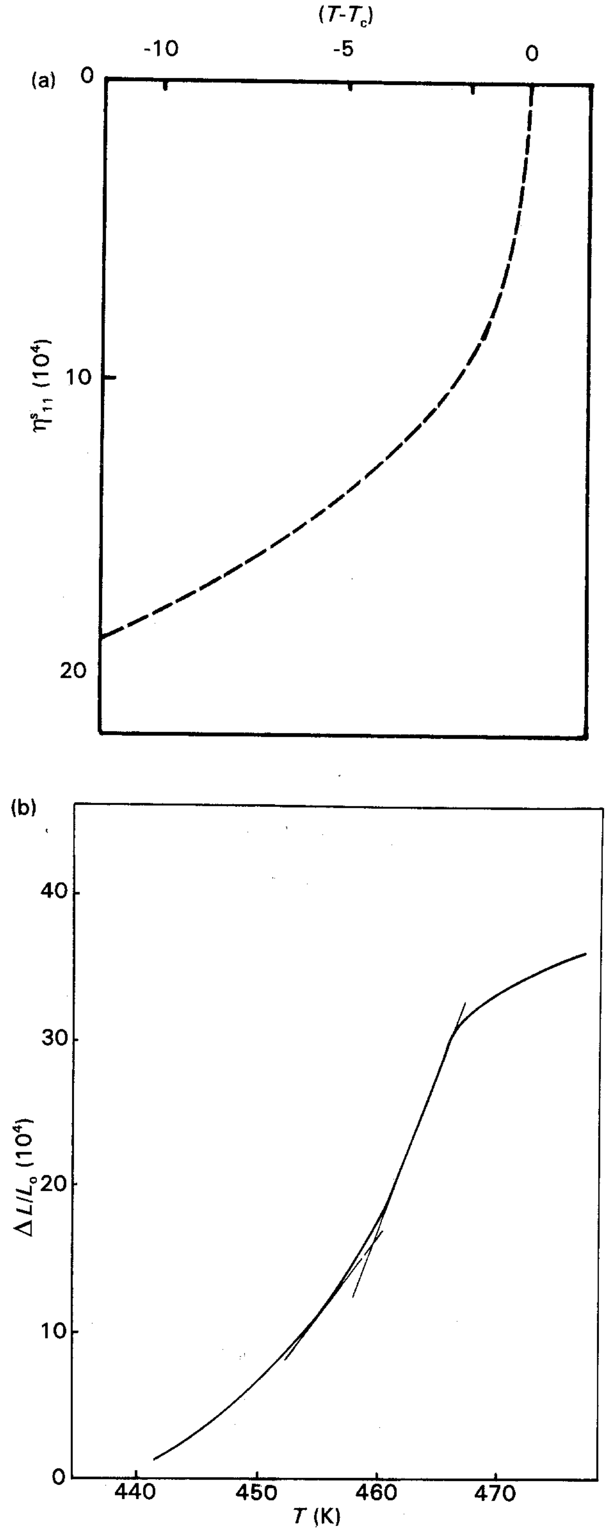

Figure 8 The temperature dependence of (a) strain and (b) elongation of LAS crystal along the x-axis in the vicinity of the α-phase transition.

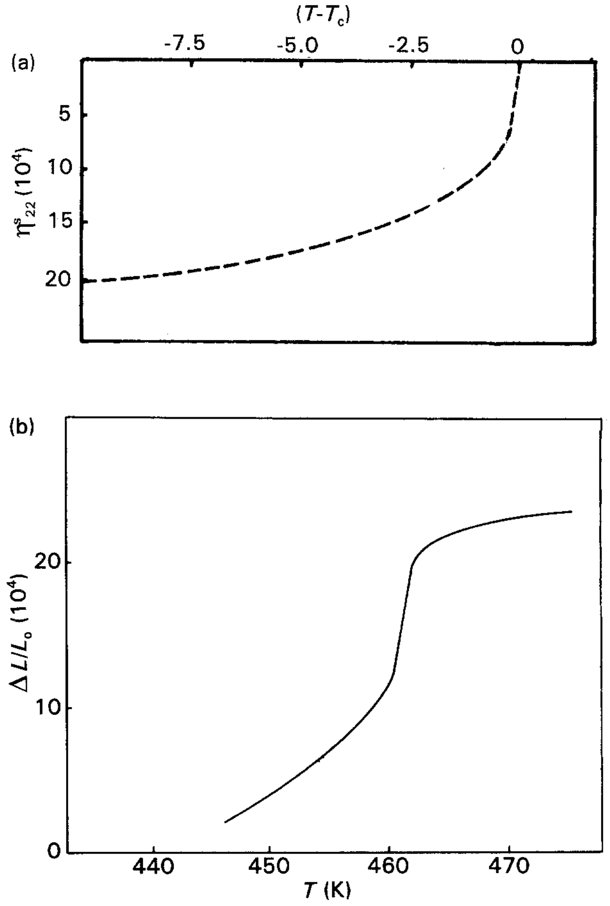

Figure 9 The temperature dependence of (a) strain and (b) elongation of LAS crystal along the y-axis in the vicinity of the α-phase transition.

interest. The corrected differential scanning calorimetry (DSC) curve of the crystal is illustrated in Fig. 4 while the temperature dependence of C_p is shown in Fig. 5. An anomaly of the specific heat typical to a first-order phase transition was observed near the transition temperature.

The specific heat, C_p, of irradiated crystals was also studied. Fig. 6 shows the temperature dependence of C_p of the irradiated samples. The maximum values of the C_p of crystals irradiated with different doses are listed in Table I. It was found that the maximum value of C_p of irradiated samples decreased with increasing irradiation doses. The decrease of the C_p with the dose was rather exponential, Fig. 7.

It is of interest to calculate the neutron doses by using the conversion factors of the International Commission on Radiological Protection [17]. Fig. 6 represents the variation of $(C_p)_{max}$ at the transition temperature versus the neutron doses, φ, in Grays (Gy). From the obtained values, one can reproduce the following empirical formula

$$(C_p)_{max} = 55.2 \exp(-0.5\varphi) \qquad (1)$$

It was assumed that the irradiation induced defects which facilitated the phase transition at 460 K, and decreased the energy involved in the transition.

It is obvious from Fig. 6 that the thermal properties are highly sensitive to the radiation effect. Accumulated radiation doses are reflected in a gradual decrease in the specific heat. Such a phenomenon could be elaborated in dosemeter applications using the Equation 1 which is valid for doses up to 2 Gy.

The enthalpy changes, ΔH, which accompanied the transition, were calculated for some irradiated samples and are presented in Table II with the corresponding entropy changes, ΔS, which were calculated from the relation $\Delta S = \Delta H/T$. The enthalpy changes, as well as the entropy changes were found to decrease with the dose.

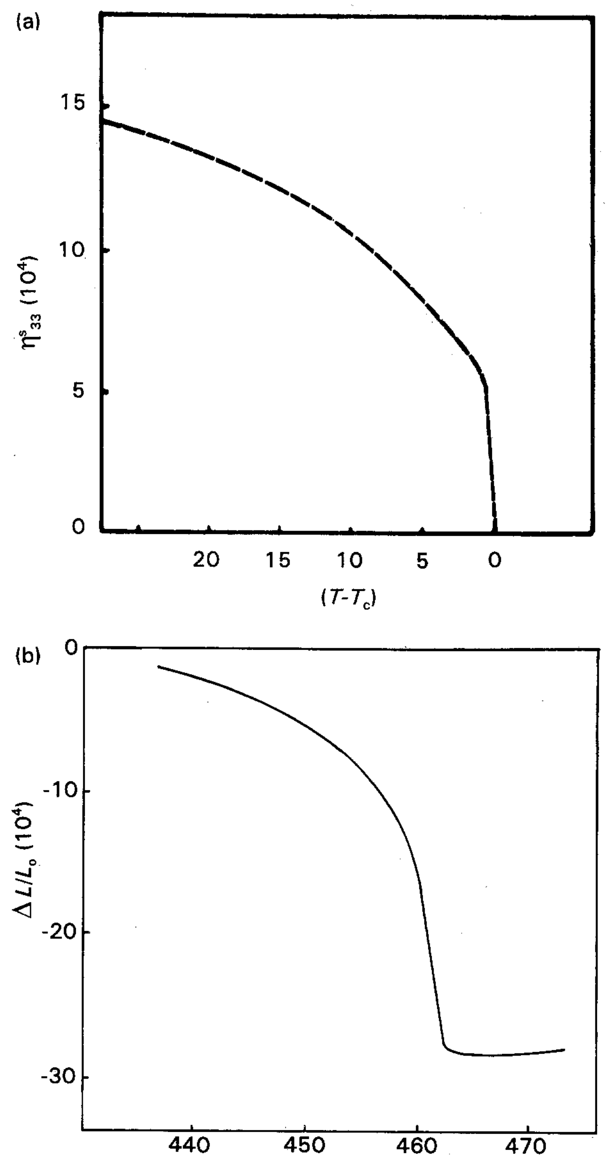

Figure 10 The temperature dependence of (a) strain and (b) elongation of LAS crystal along the z-axis in the vicinity of the α-phase transition.

TABLE III The average thermal expansion coefficient, α_{ii}, at different temperature ranges of $[\mathrm{Li}_x(\mathrm{NH}_4)_{1-x}]_2\mathrm{SO}_4$, $x = 0.5$, crystal

Temp. range (K)	α_{11} ($\times 10^{-4}$)	α_{22} ($\times 10^{-4}$)	α_{33} ($\times 10^{-4}$)
440–465	0.556	0.332	0.282
465–470	1.326	1.820	1.974
470–490	0.135	0.105	0.057

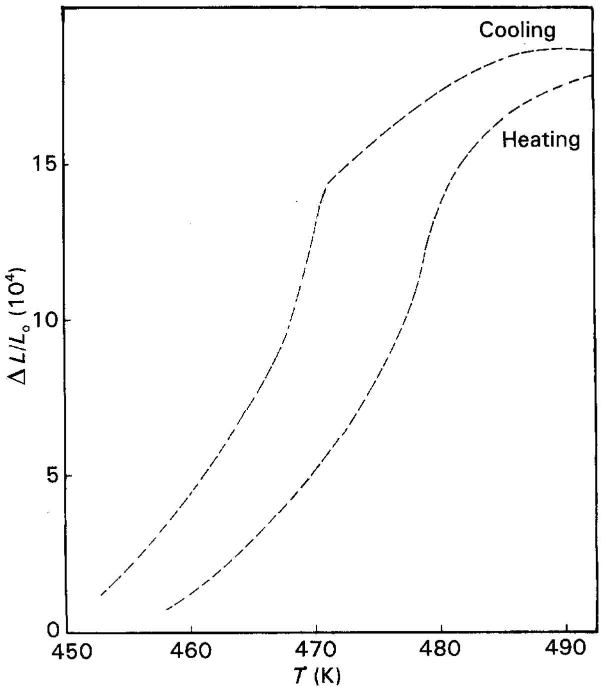

Figure 11 The thermal hysteresis of the temperature dependence of elongation on heating and cooling of LAS crystal along the x-axis.

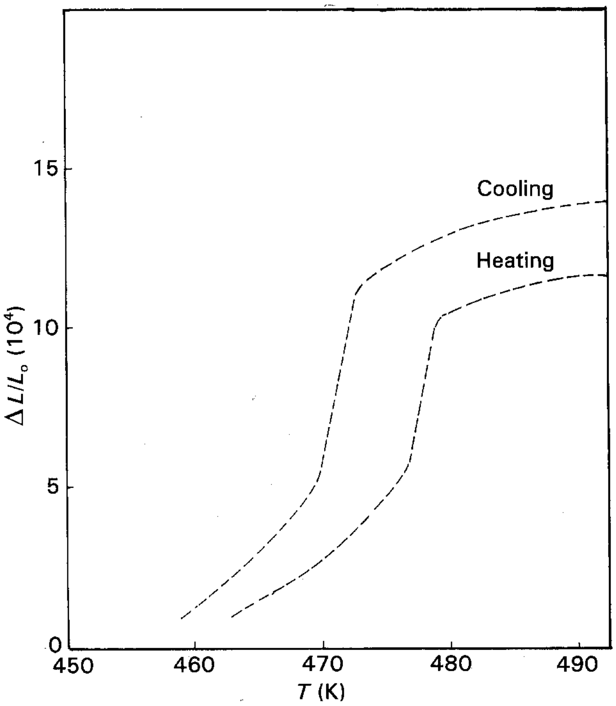

Figure 12 The thermal hysteresis of the temperature dependence of elongation on heating and cooling of LAS crystal along the y-axis.

3.2.2. Thermomechanical analysis

The temperature dependence of $\Delta L/L_0$ along the three crystallographic axes in the vicinity of the α-phase transition was measured precisely within the temperature range 440–490 K. Figs 8–10 show the dimensional changes and the transitions which occurred, while Table III gives the average thermal expansion coefficients, α_{ii} at different temperature ranges. It was clear from the figure that $\Delta L/L_0$ showed clear changes at T_c (elongation along a- and b-axes and contraction along the c-axis). This behaviour is in agreement with the results of Shimizu *et al.* [18] and Aleksandrov *et al.* [19].

The overall expansion is positive in the x- and y-axes but negative in the z-axis. The expansion is almost represented by straight lines interrupted by the anomalies at T_c. The straight lines showed different slopes. The temperature dependence of the thermal expansion coefficient in the temperature range of interest was found to be anisotropic.

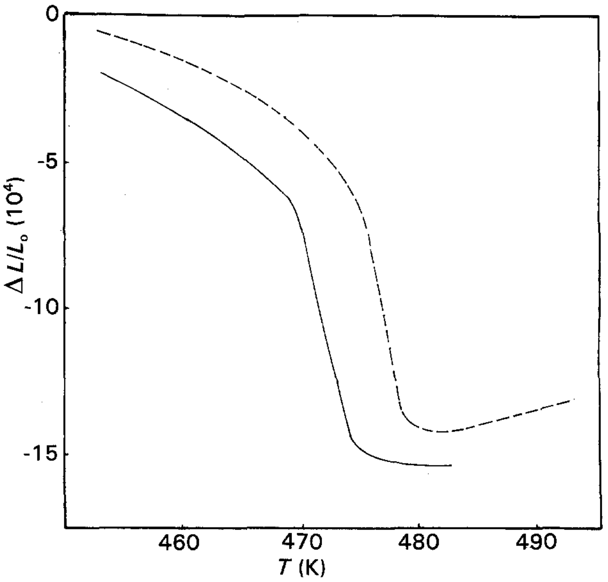

Figure 13 The thermal hysteresis of the temperature dependence of elongation on (– – –) heating and (——) cooling of LAS crystal along the z-axis.

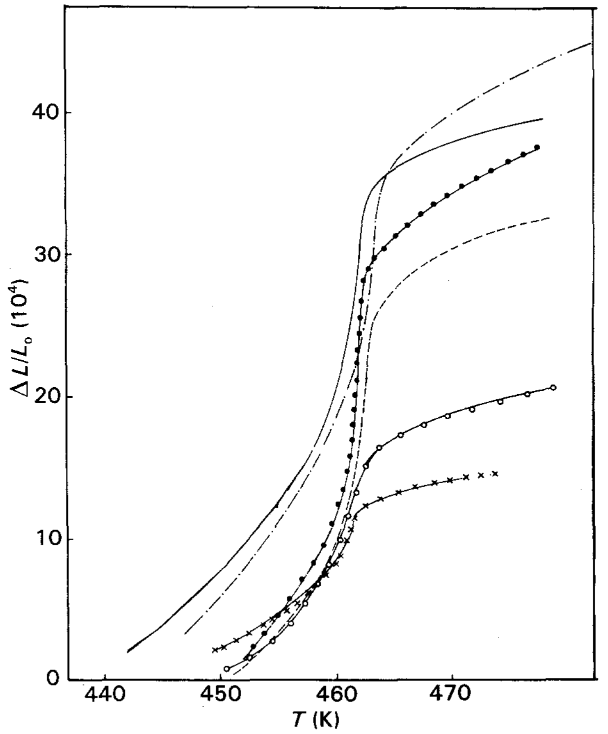

Figure 14 The temperature dependence of elongation of irradiated LAS crystal along the x-axis. Dose (10^{10} n cm^{-2}): (– – –) 0, (×) 0.432, (○) 1.296, (●) 1.944, (——) 2.700, (—·—) 3.888.

The difference between the observed value of $\Delta L/L_0$ at each temperature and that obtained by linear extrapolation from the high-temperature side is regarded as the spontaneous part induced by the phase transition [20]. Figs 8–10 also show the temperature dependence of spontaneous strain in the three crystallographic axes. The change of the spontaneous strain was found to be typical to a first-order phase change.

The hysteresis behaviour on heating and cooling in the three crystallographic axes is illustrated in Figs 11–13. The crystal showed a thermal hysteresis of about eight degrees on heating and cooling, which is one of the characteristic features of the first-order phase transition. This thermal hysteresis could be attributed to the domain-wall motions.

The samples of LAS crystals showed different thermal expansion behaviour when irradiated with different neutron doses ranging from 0 up to 3.9

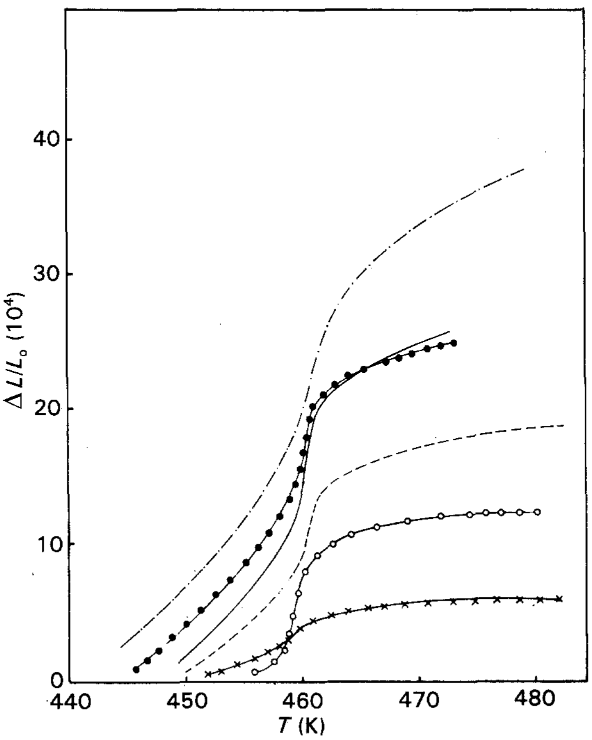

Figure 15 The temperature dependence of elongation of irradiated LAS crystal along the y-axis. Dose (10^{10} n cm^{-2}): (– – –) 0, (×) 0.432, (○) 1.296, (●) 1.944, (——) 2.700, (—·—) 3.888.

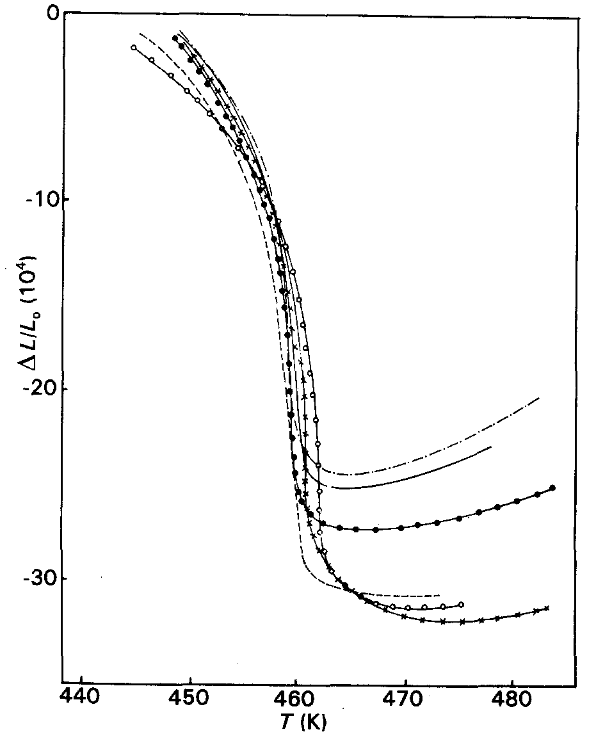

Figure 16 The temperature dependence of elongation of irradiated LAS crystal along the z-axis. Dose (10^{10} n cm^{-2}): (– – –) 0, (×) 0.432, (○) 1.296, (●) 1.944, (——) 2.700, (—·—) 3.888.

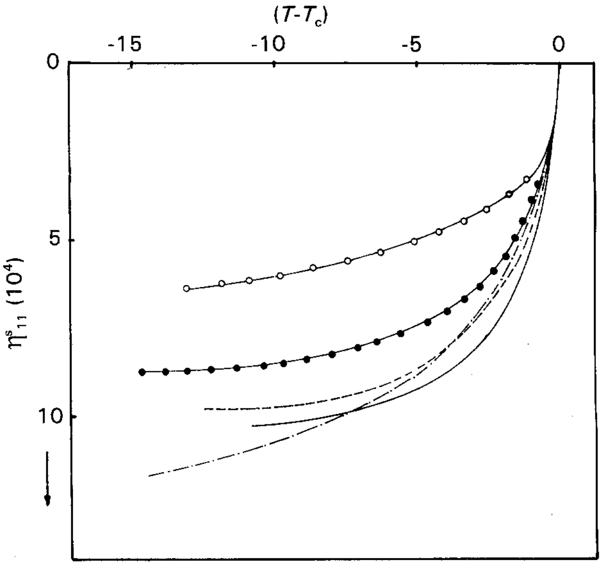

Figure 17 The spontaneous strain, η^s_{11}, of irradiated LAS crystal along the x-axis. Dose (10^{10} n cm^{-2}): (– – –) 0, (○) 1.296, (●) 1.944, (——) 2.700, (— · —) 3.888.

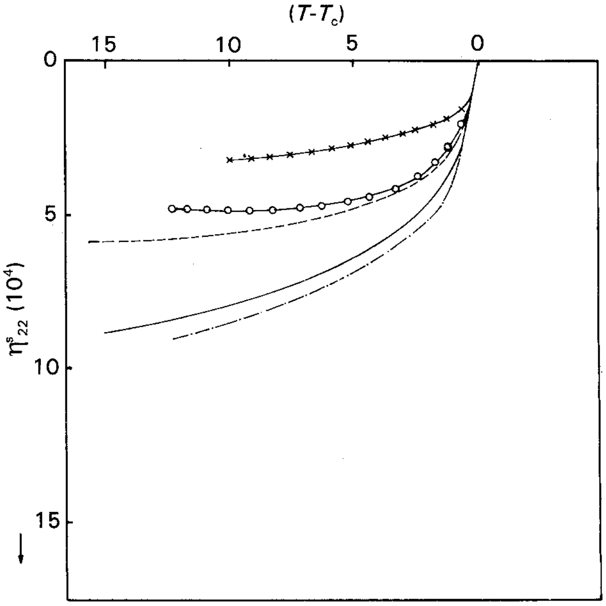

Figure 18 The spontaneous strain, η^s_{22}, of irradiated LAS crystal along the y-axis. Dose (10^{10} n cm^{-2}): (– – –) 0, (×) 0.432, (○) 1.296, (——) 2.700, (— · —) 3.888.

$\times 10^{10}$ n cm^{-2} as illustrated in Figs 14–16. The estimated values of the spontaneous tensile strains, η^s_{ii}, after irradiation are represented in Figs 17–19.

The linear thermal expansion coefficient was found to decrease with the dose up to 1.3×10^{10} n cm^{-2}, then it started to increase. It was found to be maximum when the crystal was irradiated by 3.9×10^{10} n cm^{-2} dose.

This behaviour could be attributed to the decomposition induced by irradiation, as well as the generation of new species [21]. The decomposition products may have been trapped in the interstitial positions of the crystal lattice producing stresses which clamp the domains and cause the anomaly in the crystal properties.

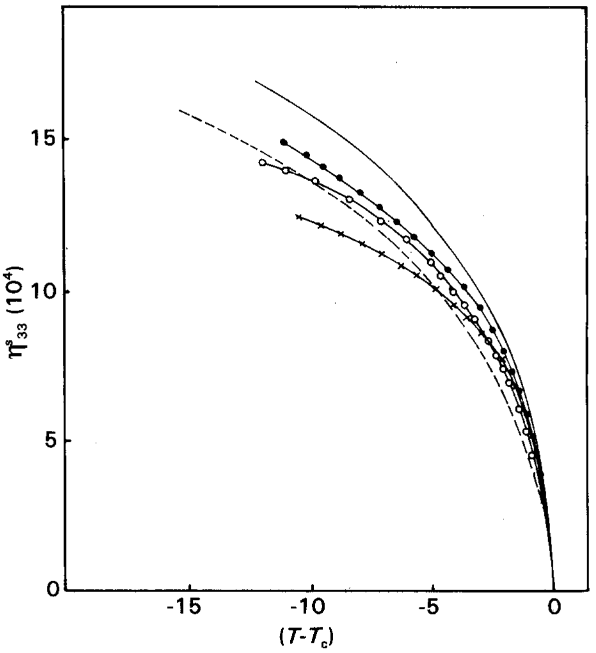

Figure 19 The spontaneous strain, η^s_{33}, of irradiated LAS crystal along the z-axis. Dose (10^{10} n cm^{-2}): (– – –) 0, (×) 0.432, (○) 1.296, (●) 1.944, (——) 2.700.

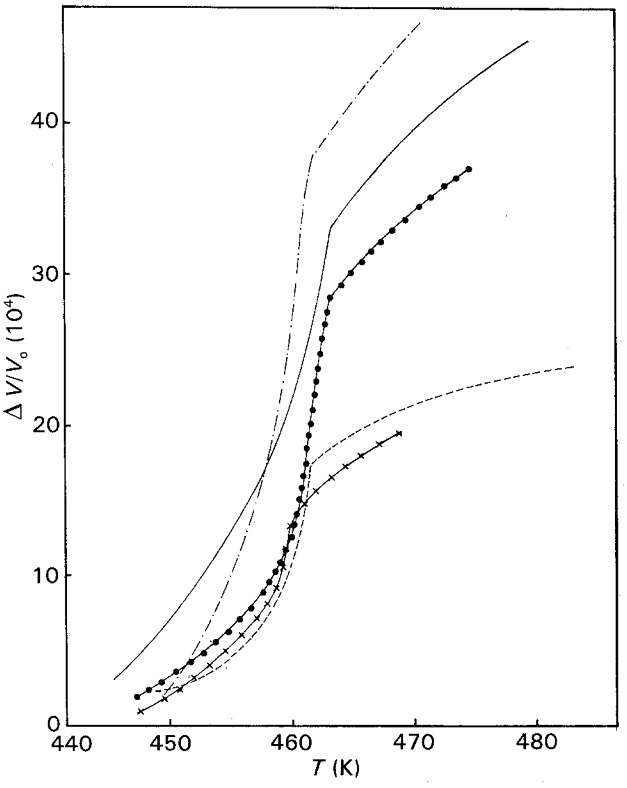

Figure 20 The volume expansion of some irradiated LAS crystal. Dose (10^{10} n cm^{-2}): (– – –) 0, (×) 0.432, (●) 1.944, (——) 2.700, (— · —) 3.888.

The results can be interpreted by assuming that two processes have taken place in the crystal lattice, namely the release of new species and the trapping process. Both processes depend on the irradiation doses. At small doses the trapping process was assumed to be non-effective and the increased concentration of generated species played the dominant role.

As the irradiation doses increased, the activity of the trapping centres became the dominant factor [22, 23].

The volume expansions, $\Delta V/V_0$, of the irradiated LAS crystals were calculated and are plotted in Fig. 20. The volume expansion of the unirradiated samples was found to be 7.23×10^{-4} at T_c, which is comparable with that estimated by Shimizu *et al.*, 6×10^{-4} [18].

The change of $\Delta V/V_0$ with temperature (the jump change at T_c) proved that the phase transition was of the first order, as illustrated by the temperature dependence of spontaneous strain as well as the temperature dependence of C_p.

4. Conclusion

It was found that impurities caused significant changes on the thermal properties of doped LAS crystals. Two-phase systems were proposed: one of the regions denoting perfect crystals and the other of regions distorted by the impurity ions (chromium, zinc and copper) therein.

The specific heat at constant pressure. C_p, of irradiated samples was found to decrease with increasing irradiation doses. This was attributed to the defects induced by the irradiation which facilitated the phase transition at 460 K. Thermomechanical analysis of irradiated samples was found to be affected by the irradiation doses. The effect of irradiation was found to be controlled by two processes: the release of new species (which was found to be dominant for small doses), and the trapping process (which was found to be dominant for higher doses). The maximum expansion was found when the crystal was irradiated by 3.9×10^{10} n cm^{-2} dose.

The volume expansion, $\Delta V/V_0$, of the unirradiated sample was found to be 7.23×10^{-4} at T_c which is in a fair agreement with the published data. The measurements also proved that the phase transition at 460 K was of the first order.

References

1. R. PEPINSKY, K. VEDAM, Y. OKAYA and S. HOSHINO, *Phys. Rev.* III (1958) 1467.
2. T. MITSUI, T. OKA, Y. SHIROISHI, M. TAKASHIGE, K. LIO and S. SAWADA, *J. Phys. Soc. Jpn* **39** (1975) 845.
3. A. I. KRUGLIK, *Kristallogr.* **23** (1978) 494.
4. W. C. HAMILTON, *Acta. Crystallogr.* **18** (1965) 502.
5. "International Tables for X-ray Crystallography", Vol. III (Kynoch press, Birmingham 1968).
6. K. ITOH, H. ISHIKURA and E. NAKAMURA, *Acta. Crystallogr.* **B37** (1981) 664.
7. I. M. ISKORNEV and I. N. FLEROV, *Sov. Phys. Solid State* **19** (1977) 605.
8. P. E. TOMASZEWSKI and A. PIETRASZKO, *Phys. Status Solidi (b)* **65** (1979) 467.
9. W. A. DOLLASE, *Acta. Crystallogr.* **B25** (1969) 2298.
10. S. A. MAHMOUD, N. G. GOMAA, A. M. EL-KHATIB and M. E. KASSEM, in "First Arab Symposium on Materials Science", Vol. 4, Alexandria (1987).
11. S. H. KANDIL, M. E. KASSEM, A. M. EL-KHATIB, M. A. EL-GAMAL and E. F. EL-WAHIDY, *J. Mater. Sci. Lett.* **6** (1987) 1261.
12. M. E. KASSEM, E. A. AMMAR, A. M. EL-KHATIB and E. F. EL-WAHIDY, *J. Thermal Anal.* **35** (1989) 2403.
13. M. E. KASSEM, N. G. GOMAA, A. M. EL-KHATIB and S. H. KANDIL, *Phys. Status Solidi (a)* **117** (1990) 119.
14. M. E. KASSEM, A. M. EL-KHATIB, A. E. HAMID and S. H. KANDIL, *Ferroelect. Lett.* **13** (1991) 215.
15. M. E. KASSEM, A. M. EL-KHATIB, E. A. AMMAR and M. M. DENTON, *J. Thermal Anal.*
16. A. M. EL-KHATIB, S. A. MAHMOUD and B. M. MOHARRAM, *Isotopenpraxis* **22** (1986) 7.
17. International Commission on Radiological Protection, "Data for Protection Against Ionizing Radiation from External Sources, Supplement to CRP Publication 15", ICRP Publication 21 (Pergamon Press, Oxford, 1973).
18. H. SHIMIZU, A. OGURI, N. YASUDA and S. FUJIMOTO, *J. Phys. Soc. Jpn* **45** (1978) 505.
19. K. S. ALEKSANDROV, I. P. ALEKSANDROVA, A. T. ANISTRATOV and V. E. SHABANOV, *Izv. Akad. Nauk. SSSR Ser. Fiz.* **41** (1977) 599.
20. S. SHIOZAKI, A. SAWADA, Y. ISHIBASHI and Y. TAKAGI, *J. Phys. Soc. Jpn* **42** (1977) 353.
21. T. OSAKA, *ibid.* **45** (1978) 571.
22. K. OKADA, J. A. GONZALO and J. M. RIVERS, *J. Phys. Chem. Solids* **28** (1957) 689.
23. G. M. LOIACONO, M. DEFLINO, A. SHAULOV, W. A. SMITH and M. I. BELL, *Ferroelectrics* **29** (1980) 181.

Received 20 March 1992
and accepted 24 February 1993